Geol. Soc. Malaysia, Bulletin 21, December 1987; pp. 1 – 21

Seismic stratigraphic interpretation for thin layers: case studies

KUO-AN LIN, SHI-CHI FUH and HSIUNG-MAO CHEN
Exploration & Development Research Centre
Chinese Petroleum Corporation,
Miaoli, Taiwan, ROC.

Abstract: A quantitative analysis system was developed and successfully applied in resolving thin porous sands, which could not be revealed by traditional methods.

The original seismic data was enhanced by reprocessing. The zero-phase wavelet synthetic seismograms and log information demonstrated the reliable quality of the seismic data, and provided the basis for constructing stratigraphic interpretation charts. A computer was used to locate the accurate coordinates of the peaks and the troughs of the seismic wavelets for the objective beds. The porosity-feet of the beds were estimated from the peak-to-trough amplitudes and time separations.

Two cases of thin-bed stratigraphy in Taiwan were studied by the above-mentioned methods. Both of these cases involved porous sands imbedded in shales. The porosity-feet of the sands in Case 1 vary from 2 to 10 meters, at about 2,000 meters depth; those in the Case 2 vary from 2 to 5 meters. at about 1,000 meters depth. The porosity-thickness in the two cases approximates that from drilling data. Each of the cases demonstrates that more favorable sand zones exist than those previously drilled.

INTRODUCTION

Since petroleum exploration entered the seismic stratigraphic era, the explorationist has been required to investigate more in detail variations in geological situations, especially in mature exploration provinces. However, this demand placed on the geophysicist has been difficult because of seismic wavelet resolution. Recently, seismic data could be analyzed to reveal somewhat smaller quantitative interpretations in structure and stratigraphy. A quantitative interpretation technique has been developed to compensate the wavelet resolution limitation and even to provide information regarding thickness and the lateral extent of thin strata.

Widess (1973) and Ricker (1953) developed techniques for the seismic resolution of thin beds. Nath and Meckel (1976), and Neidell and Poggiagliolmi (1977) discussed the significance of amplitude response for a thin bed. Even today, the stratigraphic interpretation of thin beds is an attractive topic for petroleum exploration.

This study attempts to utilize the quantitative analysis method based on the concepts discussed by the previous authors mentioned above for resolving several stratigraphic problems in two of the exploration provinces in Taiwan.

The cases considered in this study do not involve frontier exploration provinces, hence the problems are to locate and determine the extent of the productive zones. Consequently, the studies need to delve into the more detailed analyses of seismic amplitude , waveform, or even other seismic parameters.

Presented at GSM Petroleum Geology Seminar 1985

REVIEW IN CONCEPTS AND METHODS

Most stratigraphic reservoirs are generally thin in the vertical dimension, especially for sand lenses. or truncated sands. Hence, determining the limit of resolution of seismic data for these thin beds becomes a problem of major importance in stratigraphic interpretation.

It is difficult to process the wavelet to be an ideal Dirac-delta function, but just to be a bandlimited wavelet. Hence, is not meaningful to measure the interval transit time between the top and the bottom of a thin bed for thickness determination of the thin bed. It has been demonstrated that the zero-phase wavelets can improve resolution thereby simplifying the analysis. Most approaches of seismic character analysis are based on the assumption of the zero-phase wavelet; hence, the approach of data processing is to convert the propagating wavelet into the zero-phase wavelet.

As described by Nath *et al.* (1978), the thin bed resolution can be discussed by the fundamental model, which consists of a zero-phase wavelet convolved with two-termed reflectivity spikes separated by a time interval corresponding to the thickness of the bed. According to Widess's (1973) and Ricker's (1953) contributions, one can recognize that the composite waveform of convolving a wavelet with two spikes of opposite polarities and equal amplitudes approaches the derivative of the wavelet as the spike separation decreases to a limiting separation, that is,

$$\omega(t) * \delta[(t) - \delta(t - \Delta t)] = \omega(t) - \omega(t - \Delta t),$$

$$\lim_{t \to 0} \frac{\omega(t) - \omega(t - \Delta t)}{t} = \frac{d\omega(t)}{dt}$$

where $\omega(t)$= the zero-phase wavelet; $\delta(t)$ = the spike; Δt= the spike separation.

Kallweitt *et al.* (1977) proposed that the limit of resolution would be the apparent bed separation of the derivative wavelet.

Widess (1973) concluded that the limiting separation occurs when bed thickness is approximately equal to 1/8 of the predominant wavelength for the noise-free case, and degrades to around 1/4 of the predominant wavelength for the noise case. In the limiting separation,the composite waveform asymptotically approaches a constant value in the peak-to-trough time, (ΔT), and has a maximum value in amplitude, (ΔA). The limiting separation is also known as the "tuning thickness".

Figure 1 illustrates the seismic responses of 8-64 Hz bandpass wavelet from a gradually-thinning porous sand imbedded in a higher acoustic-impedance host rock with equal top and bottom reflectivities and opposite polarities for Case 1 in the studies. Figure 2 shows the time-amplitude interpretation chart for Case 1. From Figure 2, one can observe that when the bed thickness is considerably greater than the tuning thickness, the measured peak-to-trough two-way time of the composite waveform is in good agreement with the true separation of the two spikes, and the normalized peak-to-trough measured amplitude (ΔA) is constant; but when the true separation continues to decrease, the measured time first deviates slightly from the true separation and then asymptotically approaches a constant value; the amplitude first increases to a maximum, then decreases to zero as a non-linear function of bed thickness.

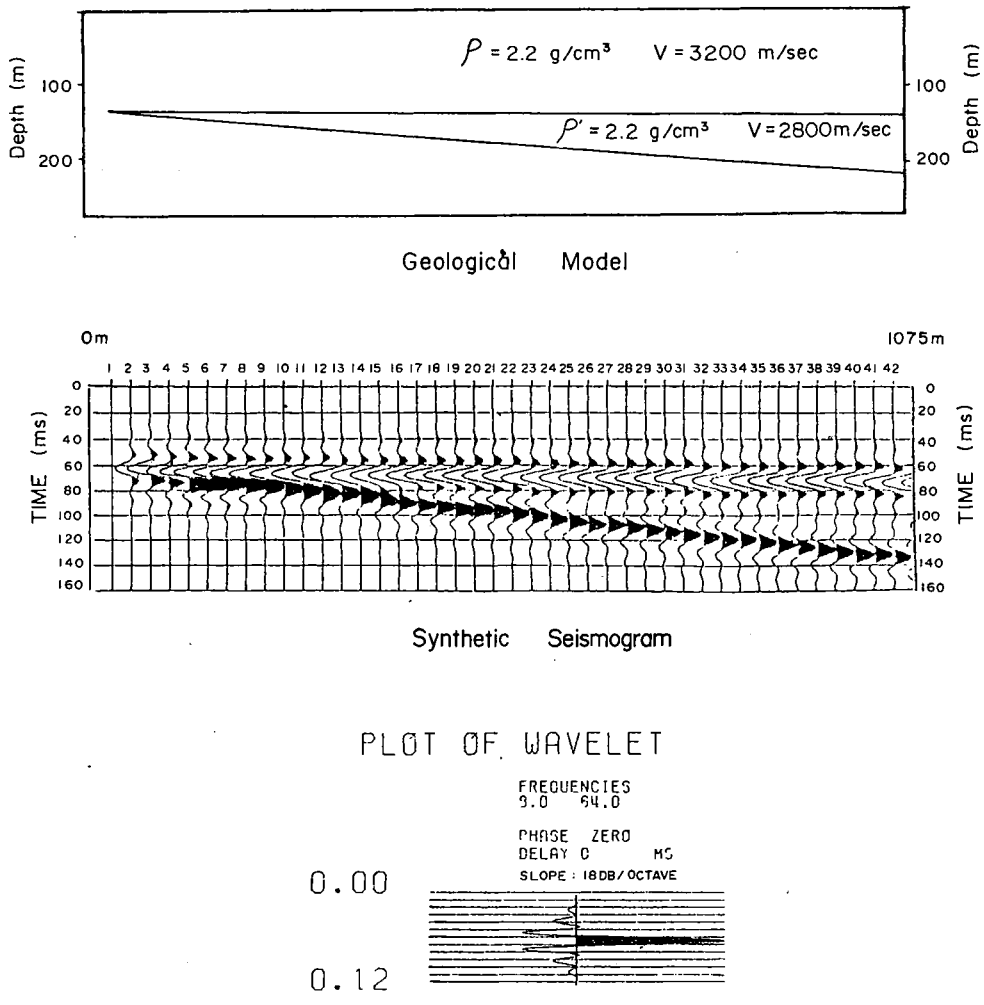

Fig. 1 Synthetic seismogram of two spikes of equal amplitude and opposite polarity

Hence, a valid bed thickness can be measured by the peak-to-trough time separation above the tuning thickness,but cannot be measured by the time separation below the tuning thickness. Instead, the bed thickness can be determined by measuring the peak-to-trough calibrated amplitude as bed thickness decreases below the tuning thickness.

The concepts reviewed above assume equal top and bottom reflection coefficients for the thin beds. However, this may not be the general case for most stratigraphic situations. When the unit overlying the thin bed and the unit underlying the thin bed have different acoustic impedances, the composite waveform of convolving the wavelet with two spikes of opposite polarities but unequal amplitudes may not approach the derivative of the wavelet as the spike separation decreases, that is,

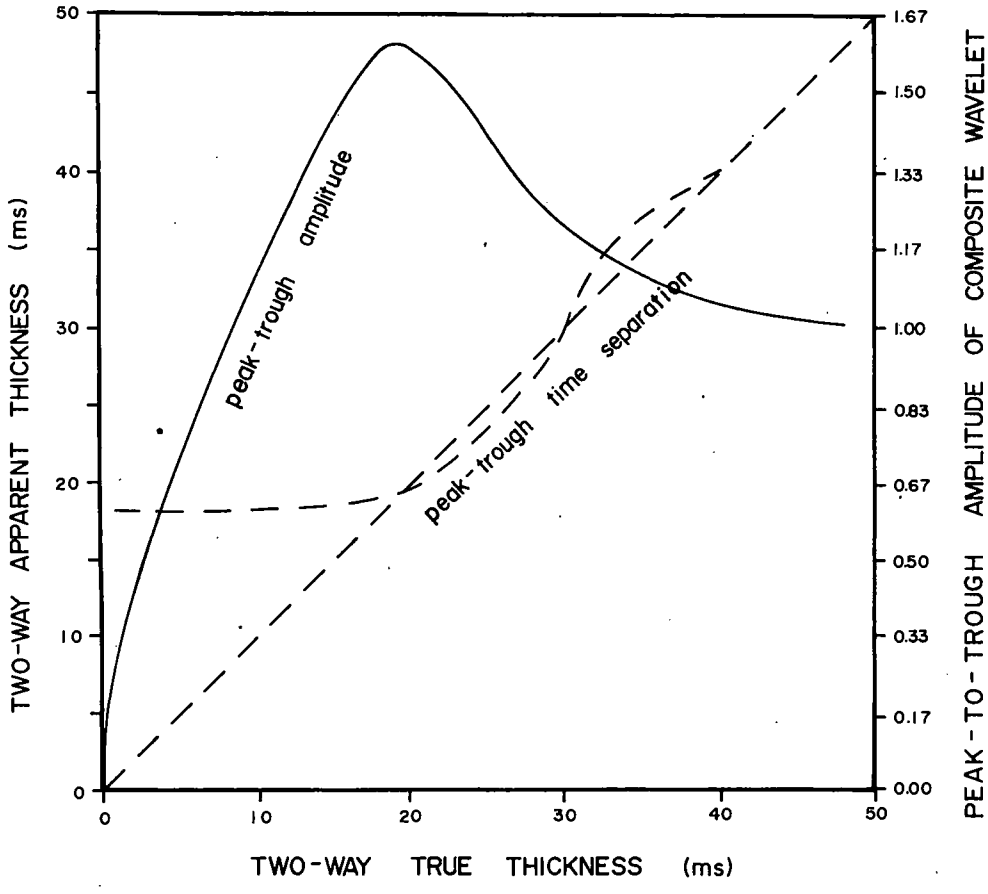

Fig. 2 Time–amplitude interpretation chart for geological model of Figure 1.

$$\omega(t) * [r\delta(t) - r\delta(t - \Delta t)] = \omega(t) - r\omega(t - \Delta t)$$

$$\lim_{\Delta t \to 0} \frac{\omega(t) - r\omega(t - \Delta t)}{t} \neq d\omega(t)/dt,$$

where r is the normalized reflection coefficient. Hence, the limit of resolution may not be the apparent separation of the derivative wavelet. Figure 3 illustrates a study of seismic responses of a 12 -to 50-hertz bandpass wavelet from a gradually-thinning porous bed of opposite polarities but unequal reflectivities for Case 2 in the study.

Figure 4 shows the plot of the peak-to-trough time separation and the peak-to-trough amplitude versus the time thickness of the thin bed. From Figure 4, it is evident that as the bed becomes thinner, the variations in amplitude and time separation have similar shapes as the variations in Case 1 for equal amplitudes, but the amplitude does not decrease to zero as

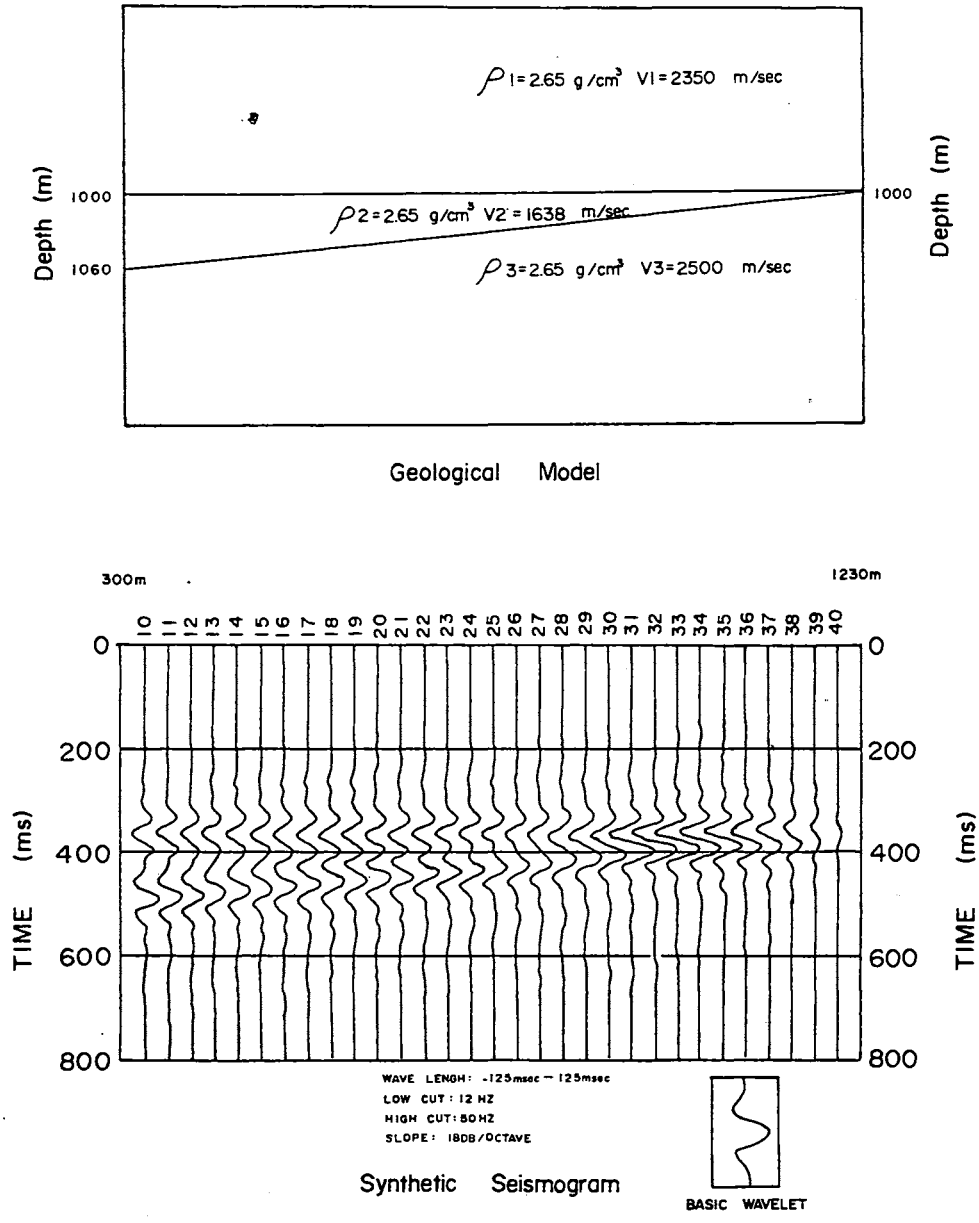

Fig. 3 Synthetic seismogram of two spikes of unequal amplitude and opposite polarity.

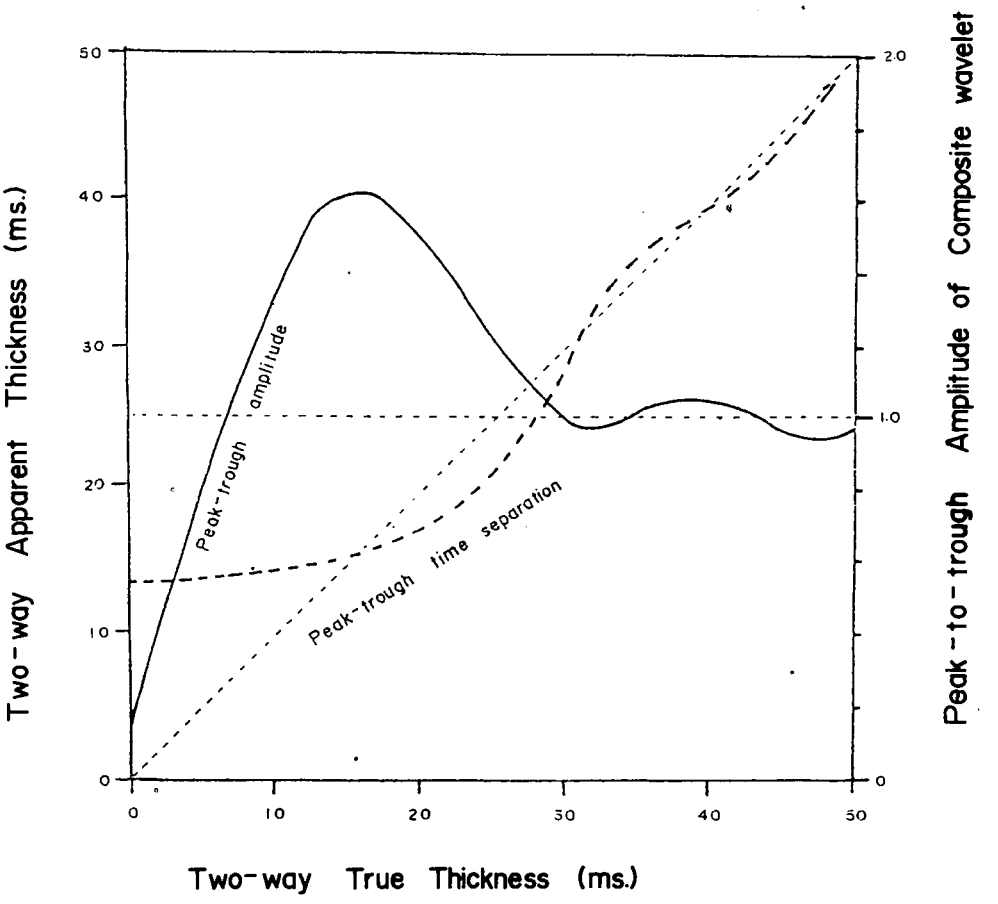

Fig. 4 Time–amplitude interpretation chart for geological model of Figure 3

the bed thickness decreases to zero. However, the curve illustrating that the amplitude decreases to a non-zero value from its maximum and is still a nonlinear function of the bed thickness, hence, it can be used for estimating the thickness of thin bed by a similar method as in Case 1.

The quantitative interpretation procedure used in the studies is illustrated in Figure 5. The major steps in the procedure are as follows : (1) obtain seismic data which has been wavelet processed,migrated and calibrated against well log(s) or other lithologic information, (2) check the quality of the seismic data with synthetic seismograms from a zero-phase wavelet and log information, (3) measure and plot time separation and amplitude curves along the seismic events encompassing the objective thin bed, (4) generate and examine the time-amplitude interpretation chart with the zero-phase wavelet extracted from the processed data, (5) edit amplitude curves within reasonable limits, (6) establish an amplitude-to-thickness scale between the tuning thickness and zero thickness points and (7) contour the thickness values.

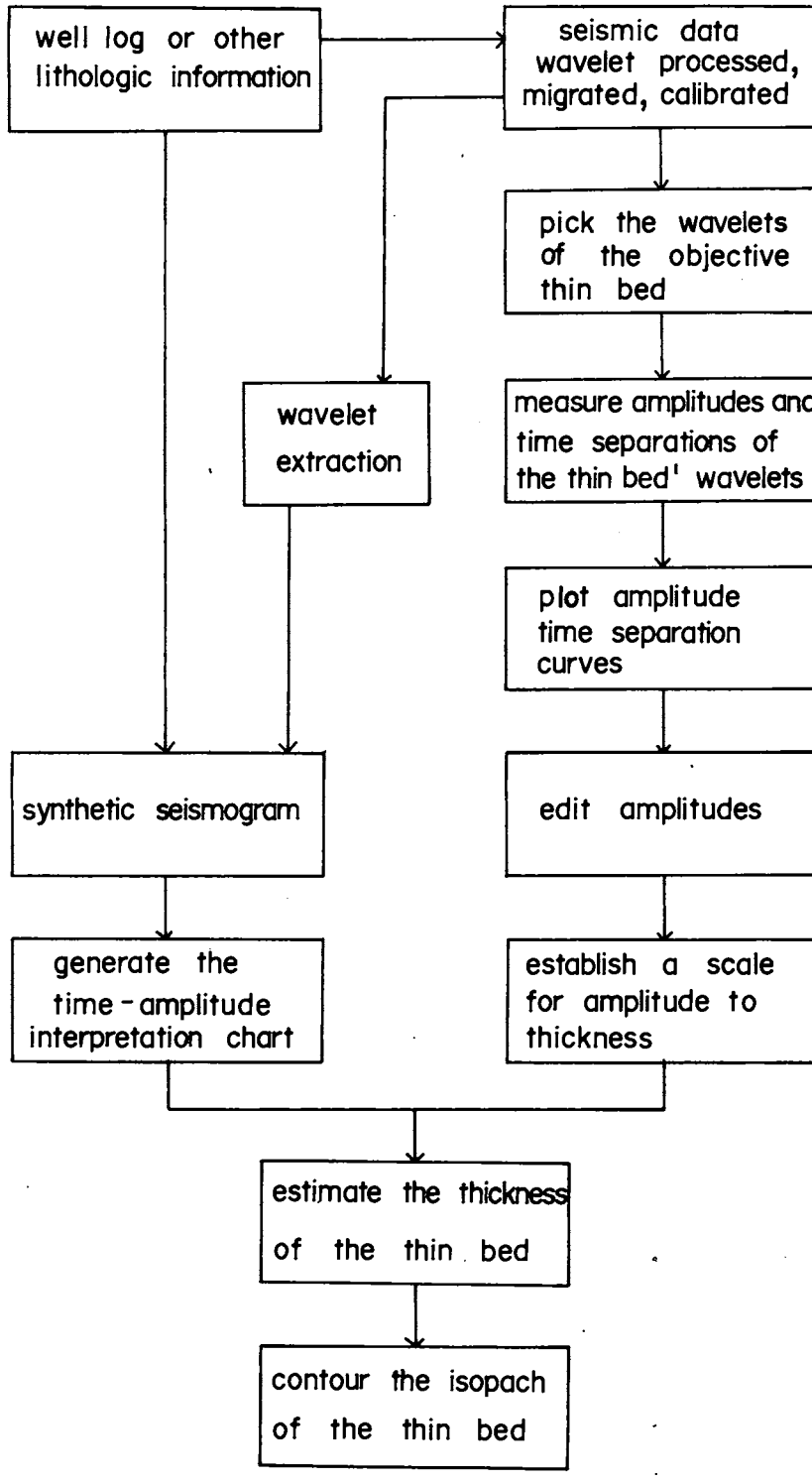

Fig. 5. Block diagram of quantitative analysis.

EXAMPLES OF TECHNIQUE

The two cases in the studies are actual examples of the practical uses of thin-bed stratigraphy for quantification of gas-saturated sandstones in Taiwan. In both of the cases, the porous sand are encased in the host shales. One can assume two-termed reflectivity spikes, which are of opposite polarities and have equal (Case 1), or unequal (Case 2) amplitudes.

Seismic grids were shot for the two areas in the study. However, portions of the lines, in which the amplitudes of reflections from the objective beds were anomalous,were selected to be analyzed. In order to define the distribution. the thickness and the potential of possible gas-bearing sands, the seismic data were reprocessed, especially for wavelet corrections. All of the seismic lines used to make the interpretations are shown in Figures 8 and 11.

In order to demonstrate the quality of the processed seismic data before making the quantitative analysis, the synthetic seismograms from log informations were generated by using the zero-phase wavelets for comparison with the processed sections. Figures 6 and 9 for Case 1 and Case 2 respectively show the acceptable correlations between the processed seismic events encompassing the objective sands and the associated synthetic seismograms. Besides, the positions of the wells were used to calibrate the amplitude data.

Figures 7-1 through 7-4 show several plots of the time-amplitude measurements of the objective sand along seismic lines for Case 1 (see the base map in Figure 8). Each of Figures 7-1 to 7-4 includes : (1) an expanded display of the seismic events, for which the peak-to-trough amplitude (ΔA) and time separation (ΔT) have been automatically measured and (2) a plot of the ΔA and the ΔT (from(l)) of the objective sand at approximately 1.6 seconds for Case 1. Figure 8 shows the distribution and.the thickness of the porous sand in Case 1, constructed from the plots of the ΔA and the ΔT as Figures 7-1 to 7-4, and based upon the interpretation chart in Figure 1. Three wells were drilled in the prospect area of Case 1. Well K-l showed the presence of an 11-meter thick net gas sand within an IS-meter sandstone, named the Talu Sand, at –l910 meters depth. Wells K-2 and K-3 encounted no net gas sands. Figures 7 and 8 indicate that the gas-filled sand in Well K-1 presents a stronger amplitude anomaly, Well K-2 and Well K-3 do not show the amplitude anomalies. Figures 7 and 8 also indicate that there is a potentially porous sand with the highest amplitude anomaly and the widest extent distributed over the area southeast of the Well K-1. There is good agreement between the seismic quantitative analysis and the drilling information, as shown in Figure 8.

Figures 10-1 through 10-4 depict several plots of the time amplitude measurements of the objective sands along the seismic lines in the area for Case 2 (see the base map in Figure 11). Each of Figures 10-1 to 10-4 also includes : (1) an expanded display of the seismic events and (2) a plot of the ΔA and the ΔT (from (1)) of the objective sands, at approximately 1 second in Case 2. Figure 11 shows the distribution and the thickness of the porous sand in Case 2, estimated from the plots of ΔA and ΔT in Figures 10-1 to 10-3, and based on the interpretation chart in Figure 2. The prospect area in Case 2 includes three wells, which had been drilled in updip positions. Well HSY-l showed the presence of a 2.5-meter thick net gas sand within the Erchungchui Formation , at -1017 meters. The other two wells, HSY-2 and HSY-3, encountered a l-meter thick muddy sand at –1034 meters and a 3-meter thick muddy sand at –998 meters, respectively.

Figures 10 and 11 indicate that the net gas sand in Well HSY-1 presents a considerably

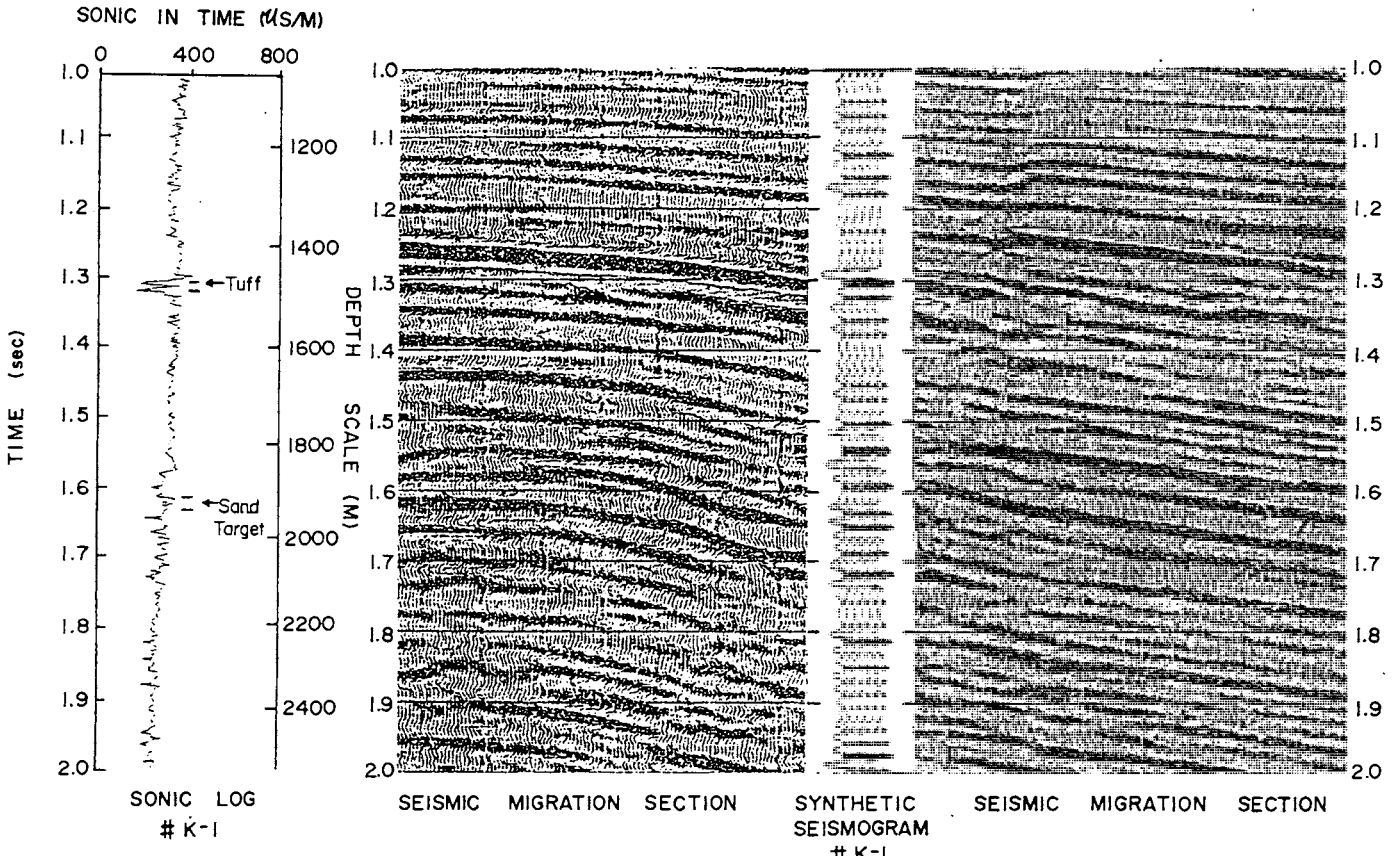

Fig. 6. Correlation of seismic section of Line I with the synthetic seismogram from Well K-1 located at Line I in Case I

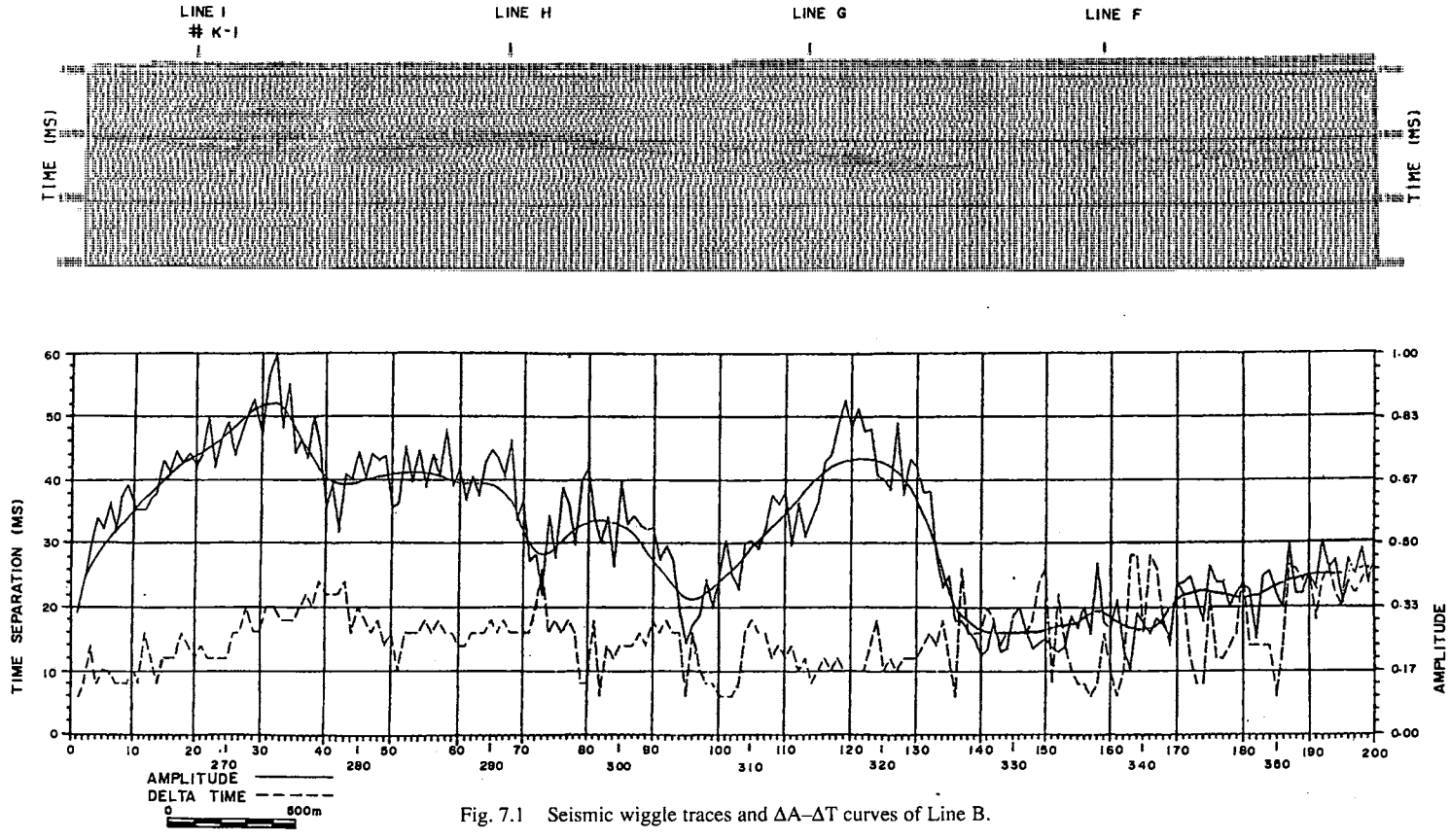

Fig. 7.1 Seismic wiggle traces and ΔA–ΔT curves of Line B.

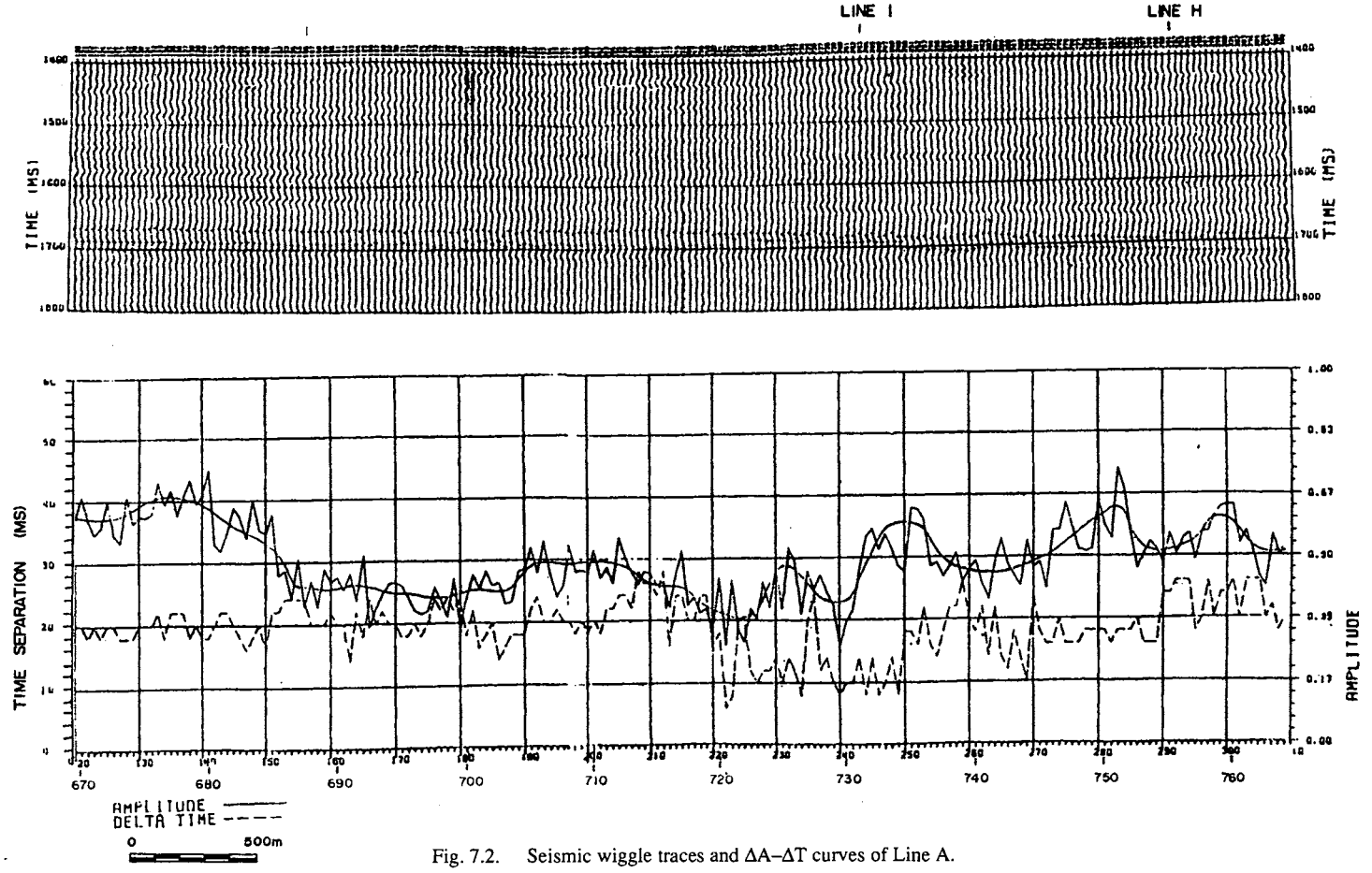

Fig. 7.2. Seismic wiggle traces and ΔA–ΔT curves of Line A.

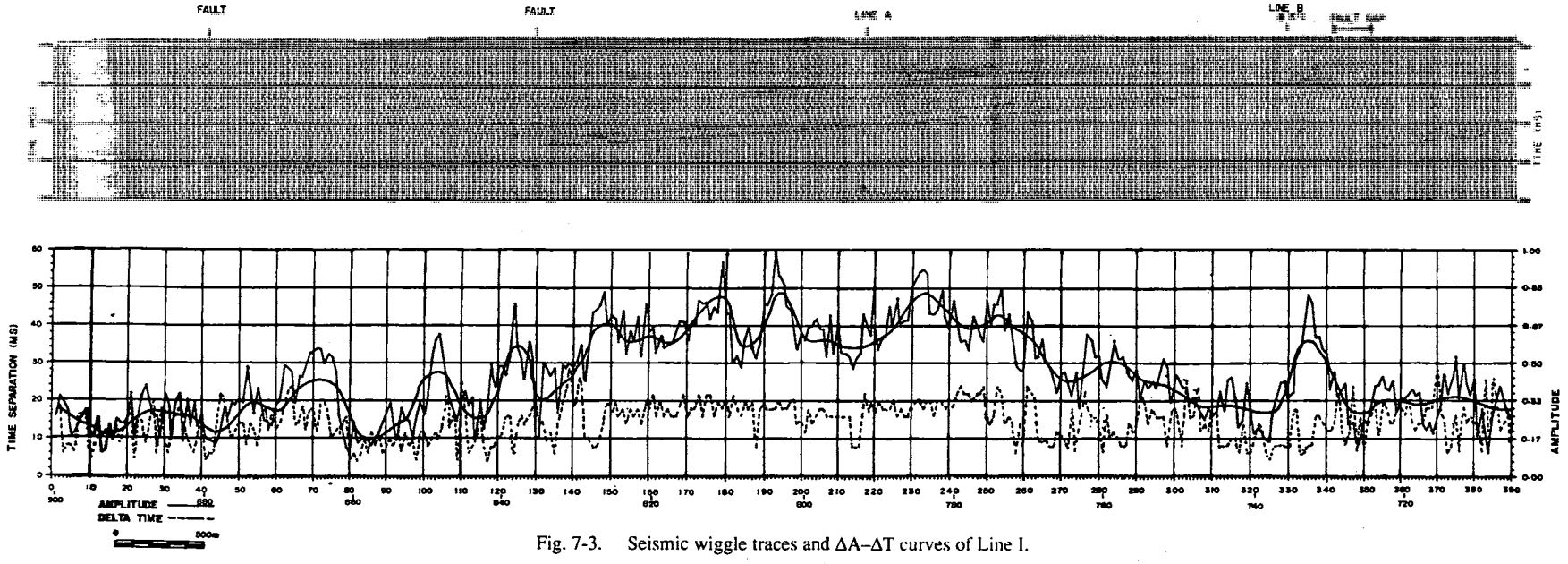

Fig. 7-3. Seismic wiggle traces and ΔA–ΔT curves of Line I.

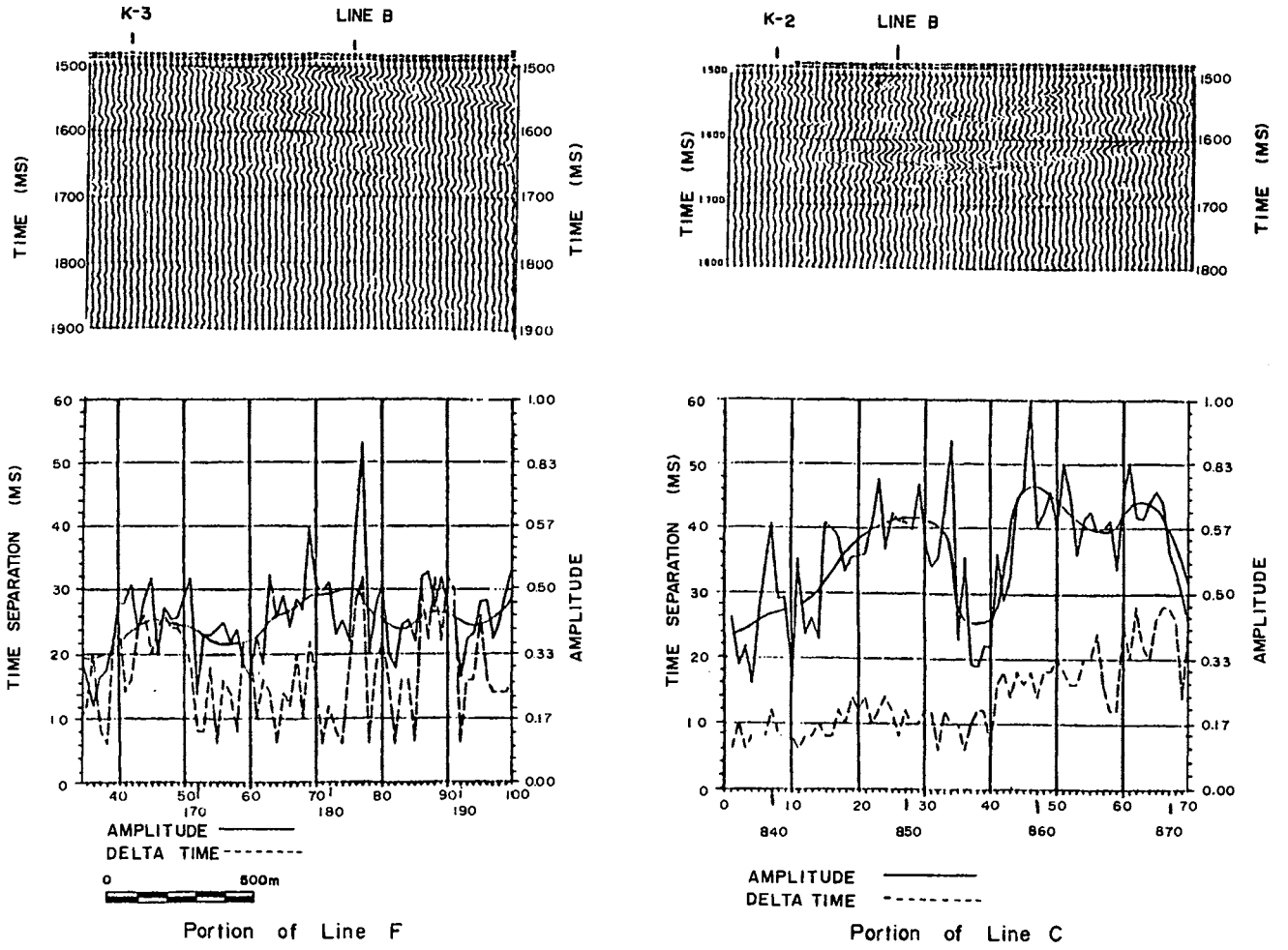

Fig. 7-4. Seismic wiggle traces and ΔA ΔT curves of portions of Line F and Line C.

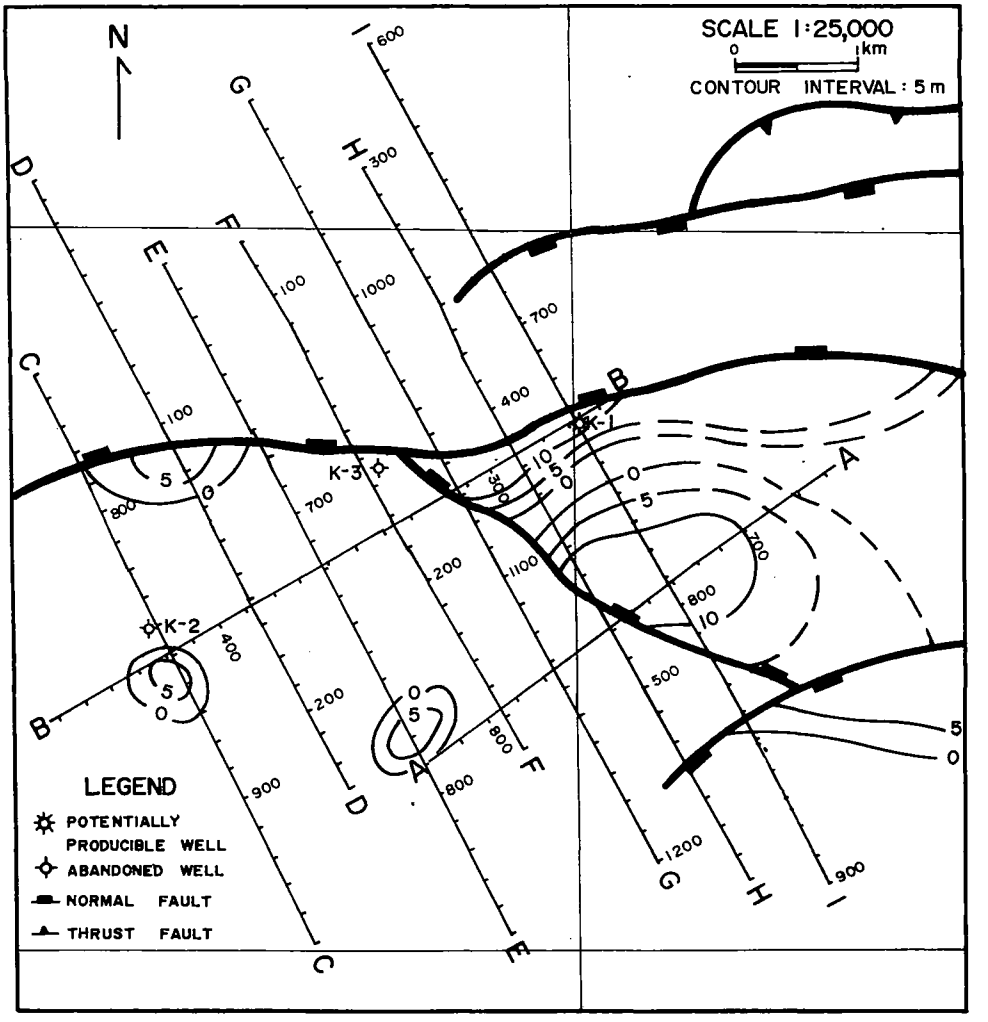

Fig. 8. The isopach of the porosity-feet of porous sand (Talu Sand) in Case 1.

higher amplitude anomaly; the muddy sands in Wells HSY-2 and HSY-3 do not have high amplitude anomalies associated with them. Figure 11 also indicates a potential porous sand body with the greatest amplitude anomaly and the largest lateral extent distributed over the area east and northeast of Well HSY- 1. Figure 11 shows the satisfactory agreement between the drilling data and the quantitative interpretation.

CONCLUSIONS

The quantitative interpretation could provide the explorationist with more detailed information about stratigraphic variations. Several non-geologic factors affecting the accuracy

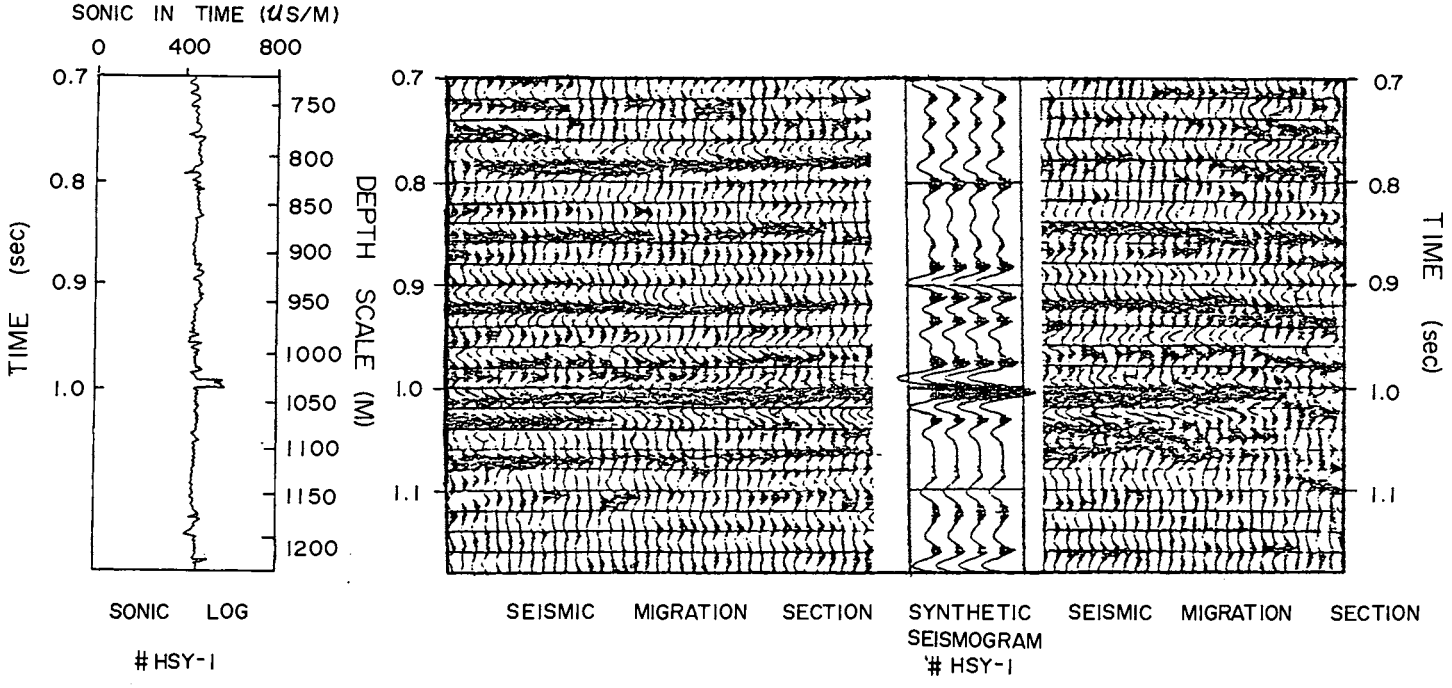

Fig. 9. Correlation of seismic section of Line DA with the synthetic seismogram from Well HSY-1 located at Line DA in Case 2.

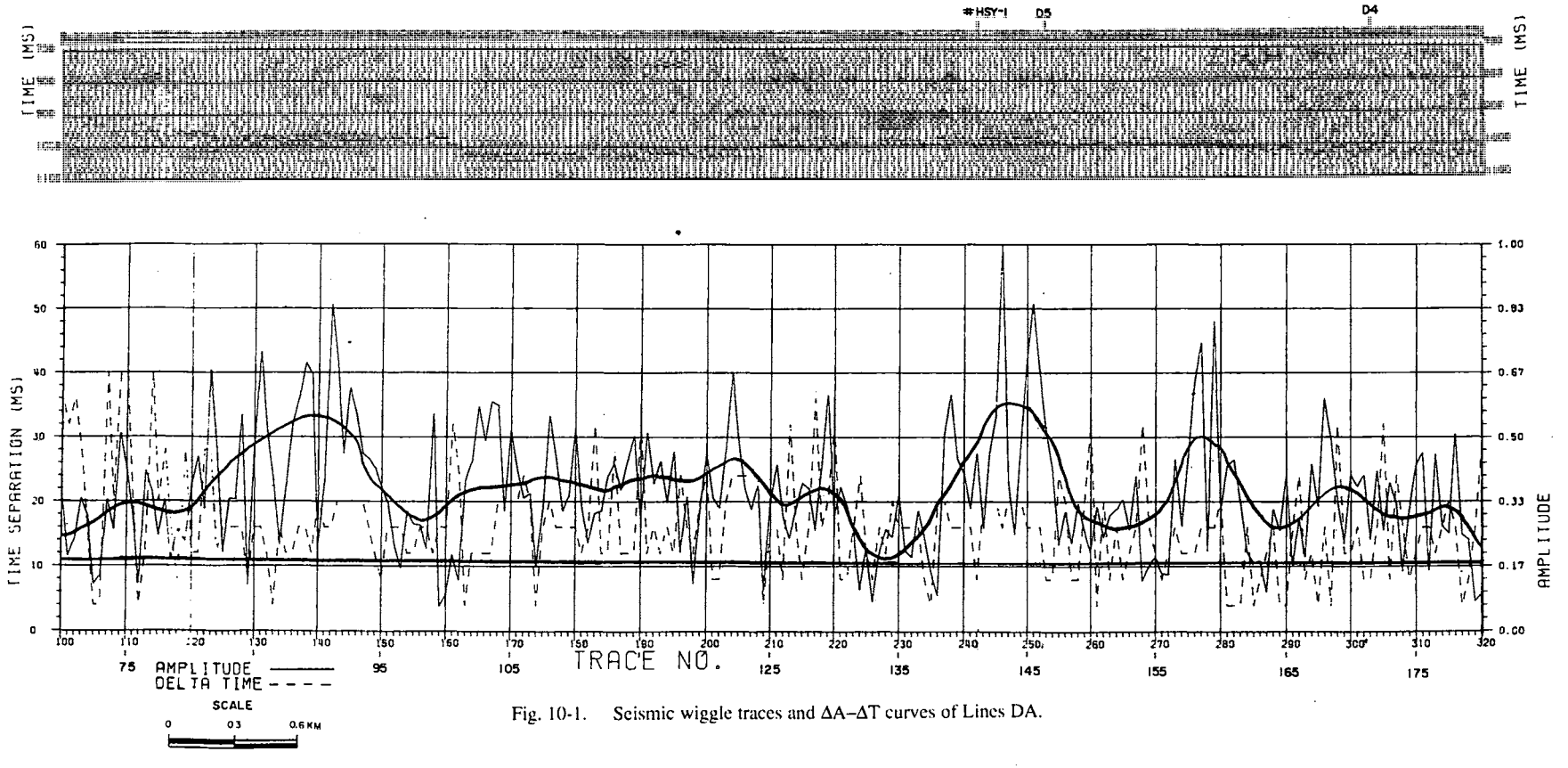

Fig. 10-1. Seismic wiggle traces and ΔA–ΔT curves of Lines DA.

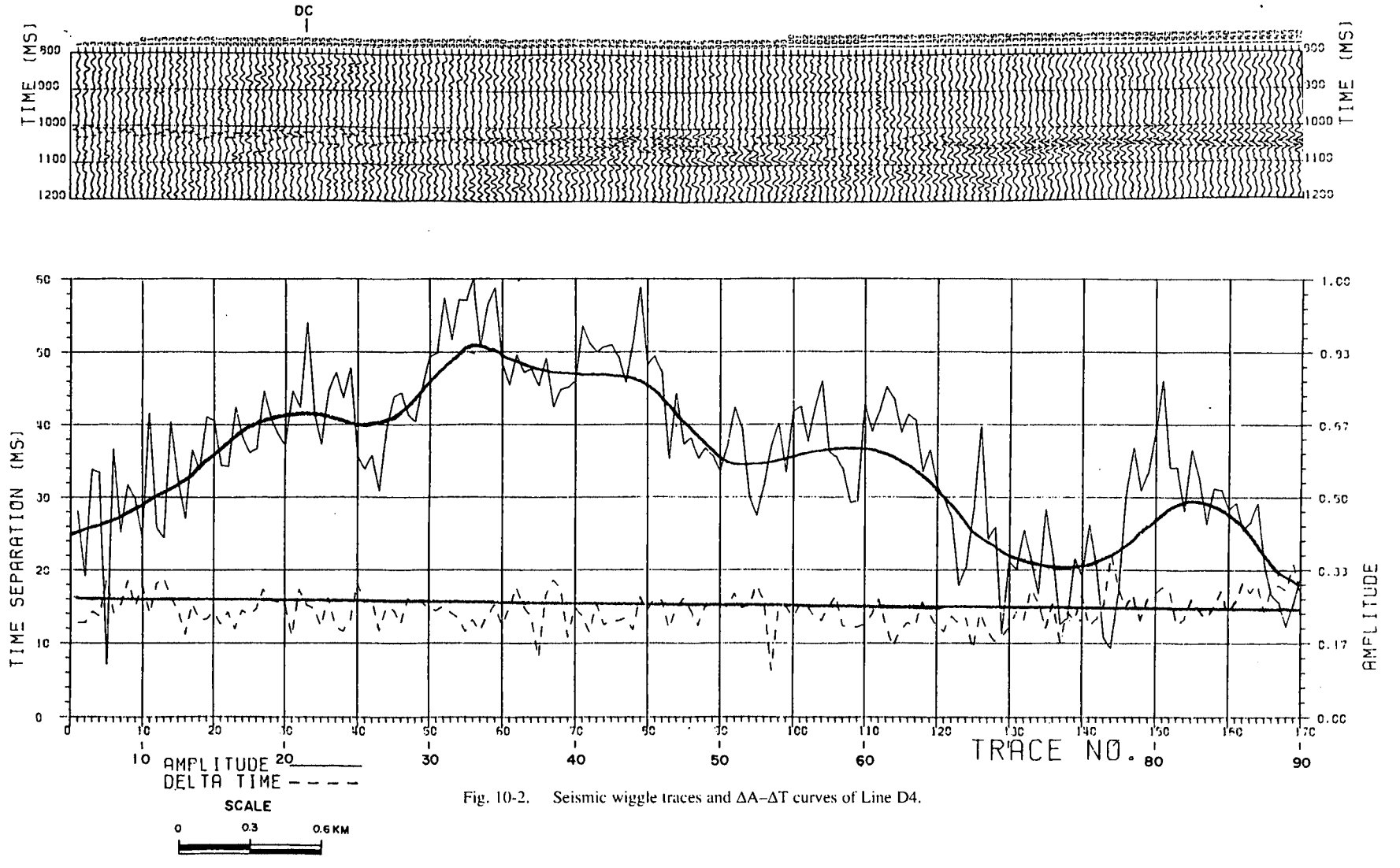

Fig. 10-2. Seismic wiggle traces and ΔA–ΔT curves of Line D4.

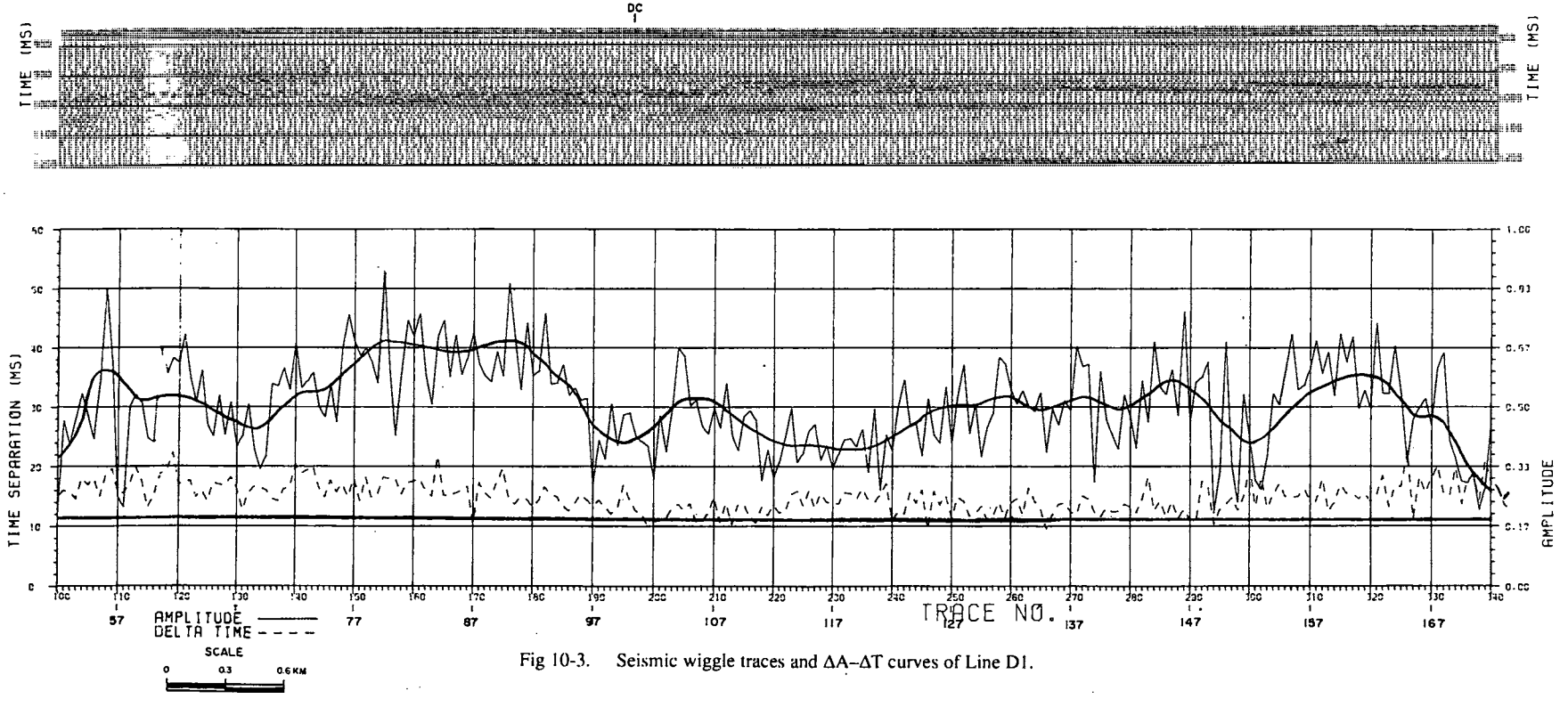

Fig 10-3. Seismic wiggle traces and ΔA–ΔT curves of Line D1.

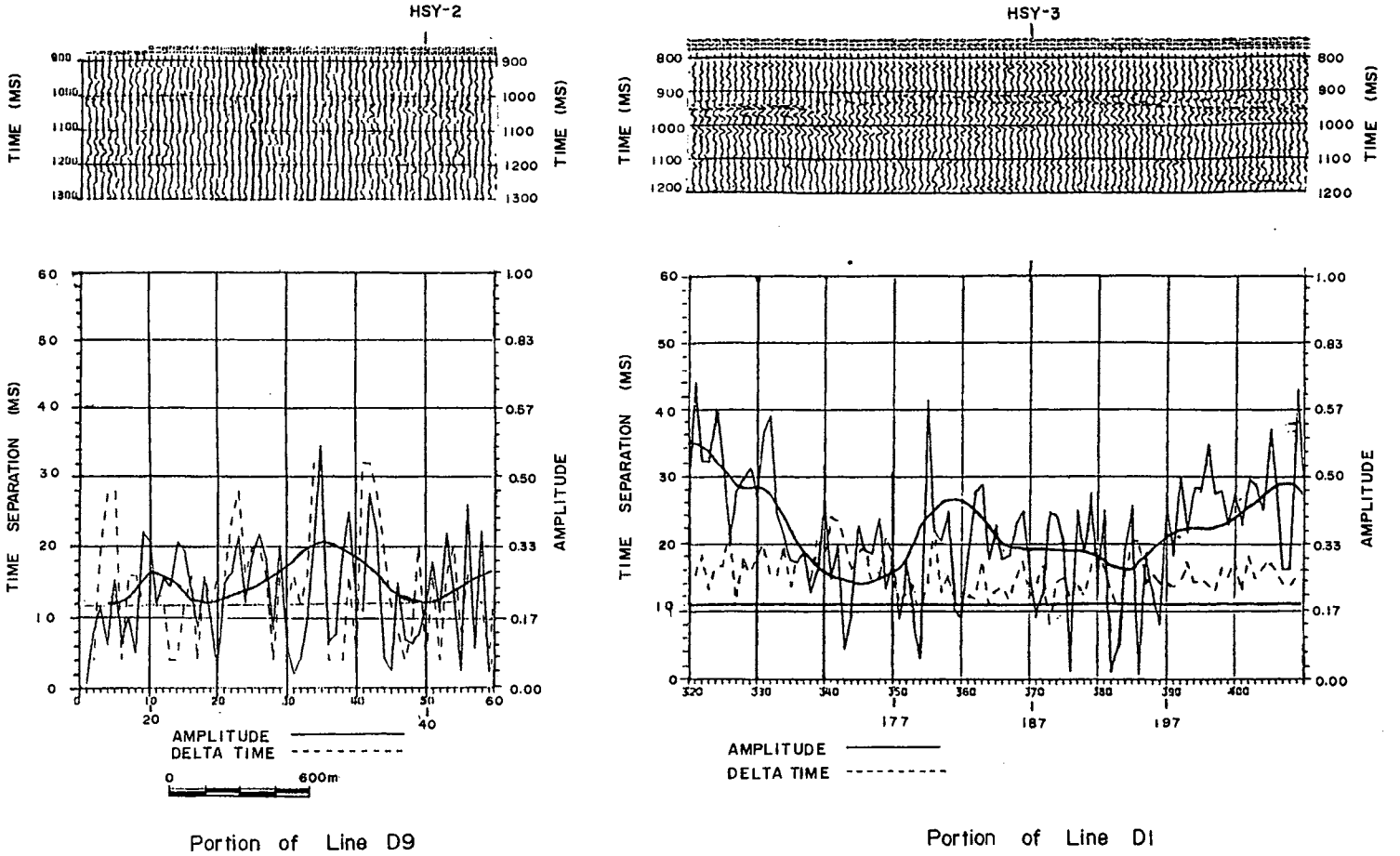

Fig. 10-4. Seismic wiggle traces and ΔA–ΔT curves of portions of Line D9 and Line D1.

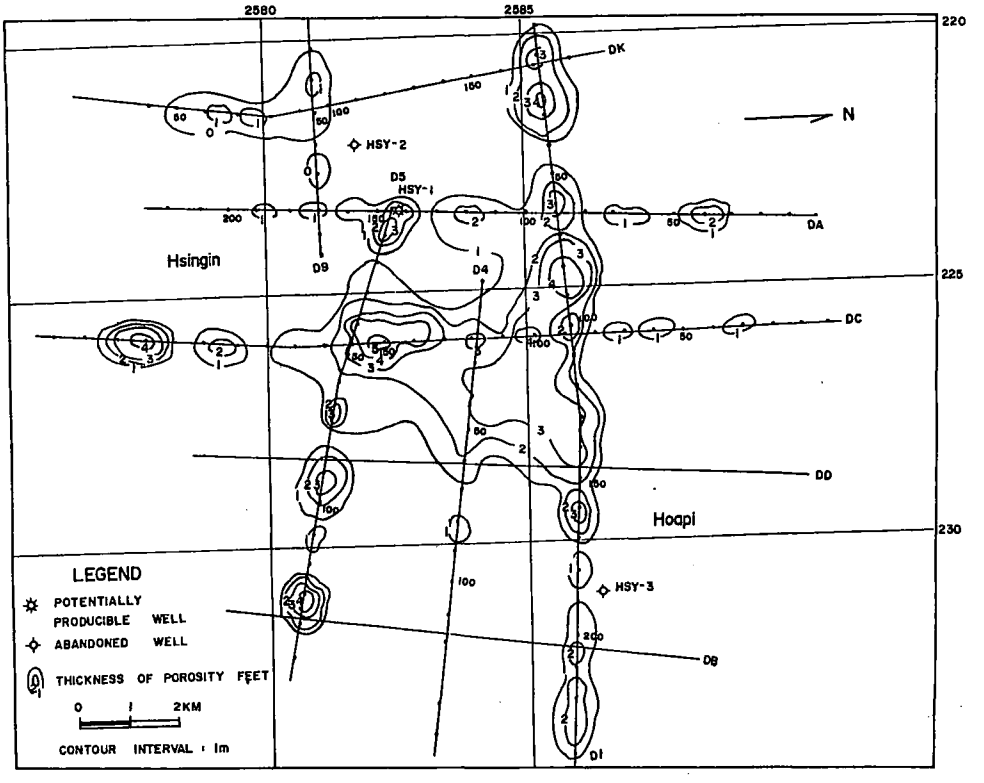

Fig. 11. The isopach of the porosity-feet of porous sand (Erchungchui Formation) in Case 2.

of this method should be removed carefully during data acquisition and processing. The availability of definite calibrating devices such as log information from one or more wells in the nearby area is beneficial for calibration purposes.

Porosity and thickness are the major parameters controlling the reflectivities of a thin layer. Thin high-porosity zones may have some effect as equivalent thickness with lower porosity. Porosity and thickness may vary over an exploration province; hence, the estimated thickness could be porosity-feet. However, our objective of selecting the best drilling site is achieved even though the thickness is porosity-feet.

Seismic data quality demonstrated by the synthetic seismograms and amplitude calibrations based on log information seem to imply that the potentially porous sands distributed over the area southeast of Well K-1 in Case 1 and those sands distributed over the area east and northeastof Well HSY-1 in Case 2 are worthwhile to be considered as future drill-sites.

REFERENCES

KALLWEIT, R.S., WOOD, L.C., and MOFFITT, J.R., 1977. *The Seismic Resolution of Zero Phase Wavelets*. Presented at SEG 47th Annual Meeting, Calgary.

NATH, A. K., and MECKEL, L.D., Jr. 1976. *Seismic Modeling for Structural and Stratigraphic Interpretation.* Presented at SEG 46th Annual Meeting, Houston.

NATH, A.K., and MECKEL, L.D., Jr., and WOOD, L.C., 1978. *Synergistic Interpretation of the Convolutional Model. Segment 4, The convolutional Model.* An SEG School, SEG, U.S.A..

NEIDELL, N.S. and POGGIAGLIOLMI, E., 1977. Stratigraphic Modeling and Interpretation-Geophysical principles and Techniques. *AAPG Seismic Stratigraphy Symposium, Memoir 26.*

RICKER, N., 1953. Wavelet Contraction, Wavelet Expansion and the Control of Seismic Resolution. *Geophysics*, v. 18, no. 4, p. 769-792.

WIDESS, M. B., 1973. How Thin is a Thin Bed ? *Geophysics*, v. 38, no. 8, p. 1178-1180.

Manuscript received 6 December 1985